The Water Forcefield: Importance of Dipolar and Quadrupolar Interactions†

José L. F. Abascal* and Carlos Vega

Departamento de Química Física, Facultad de Ciencias Químicas, Universidad Complutense, 28040 Madrid, Spain

Received: June 7, 2007; In Final Form: August 11, 2007

It is widely recognized that dipolar interactions play a fundamental role in water. Less emphasis is put on the effects dues to the quadrupole moment. The recent calculation of the phase diagram for several rigid, nonpolarizable water models has shown that this is a rather severe test for water potentials. In this work, we analyze the results yielded by popular three-point-charge water models (TIP3P, SPC, SPC/E, TIP4P, TIP4P-Ew, TIP4P/2005, and TIP4P/Ice) and attempt to correlate them with the molecular dipoles and quadrupoles. It is shown that the melting temperatures of the proton disordered ices depend almost linearly on the quadrupole moments. However, the relative stability of ice II with respect to ices III, V, and VI seems to be rather dependent on the ratio of dipolar/quadrupolar forces. Small departures from a given ratio increase the stability of ice II and result in a serious deterioration of the phase diagram. Simple expressions are derived for the dipole and quadrupole moments, which allow us to analyze the effect of these multipole moments in the phase diagram when the rest of the molecular parameters are fixed. Satisfactory results for both the melting temperatures and for the relative stability of the different ices are obtained only when the molecular quadrupole approaches that of the isolated water molecule. Or, expressed in terms of the model parameters, acceptable results require that the negative charge be shifted from the oxygen toward the hydrogen positions by 0.14 Å or more.

I. Introduction

Water is probably the most studied substance in nature. This is not only a consequence of its importance in our everyday life, but it is also due to its peculiar behavior which makes it the target of a great number of theoretical investigations. Both sources of interest (theoretical and practical) are closely related since many industrial and biochemical processes ultimately rely on its unusual physicochemical properties. Hence, there is interest in an adequate description of the intermolecular interactions in water. The complexity of the water properties together with the different possible levels of description have led to the proposal of hundreds of models (see the excellent review by Guillot[1] for a critical analysis of the results yielded by these models). At first, it would seem feasible that an analytical fit of ab initio calculations of the potential energy surface (PES) of water dimers could provide accurate potential functions.[2] Unfortunately, the results did not confirm the expectations. This is because the procedure has a number of limitations. The first is due to the reduced number of points used to represent the potential energy surface. Besides, since the potential energy represents only a small fraction of the total energy of the system, the precision of the calculations may compromise the results. Moreover, calculations based on the water dimer or more complex water clusters do not necessarily give an accurate representation of water in condensed phases. For these reasons, most of the popular water models are still empirical. However, promising results have been recently obtained with more refined electronic calculations. This is the case, for instance, of the MCDHO model[3] obtained from a fit of a refined ab initio single molecule deformation PES.[4] These calculations provide qualitatively important information on the interactions between water molecules. In fact, some models incorporate features obtained in ab initio calculations. For instance, in the PPC model,[5] the polarization produced by an external field or by other molecules determines the electrostatic terms of the force field, while the short-range interactions are calculated as those in empirical models, that is, they are optimized to reproduce several properties of liquid water at 298 K.

Ab initio calculations are also a source of information about the values of the dipole and higher multipole moments of the water molecule in different environments. All of the studies indicate that the mean value of the dipole moment in condensed phases is larger than that of the isolated molecule (1.85 D). However there is a nonnegligible uncertainty in these results. The first estimation of the "experimental" dipole moment of the hexagonal ice Ih (which cannot be directly measured) was 2.6 D,[6] but this estimate has been challenged by several authors. Recent calculations yield the value $\mu = 3.09$ D.[7] This result is slightly larger than the "experimental" dipole moment of liquid water at 298 K, $\mu = 2.95$ D, which has been recently reported[8] based on experimental data with some support of ab initio calculations and molecular dynamics results for popular water models. The experimental value is in the upper range of ab initio simulations of liquid water, which give a relatively large spread of values (from 2.43[9] to 2.95 D[10]) due to the different ways of assignment of the electronic density to individual molecules. It is interesting that the mean μ values calculated in simulations of polarizable water models exhibit a similar range of values.[4,11−13] Thus, a literature survey clearly indicates that the relation between the dipole moments of ice Ih, liquid water, and gas-phase water are $\mu_{ice} \geq \mu_l > \mu_g$.

High-quality quantum mechanical calculations such as those performed by Probert and reported in the book by Petrenko and Whitworth[14] show that the contour of the total electron density

† Part of the "Keith E. Gubbins Festschrift".

10.1021/jp074418w CCC: $37.00
Published on Web 10/06/2007

of water is approximately trigonal.[15] Accordingly, most of the empirical models usually place three point charges at the molecule. These successful models (SPC,[16] SPC/E,[17] TIP3P,[18,19] TIP4P[19]) are optimizations of the Bernal−Fowler[20] potential. They consist of a Lennard-Jones (LJ) site at the oxygen atom and three fixed point charges. Two positive charges are placed at the hydrogens, and the negative one is located at the oxygen (SPC, SPC/E, and TIP3P) or shifted toward the hydrogens along the bisector of the H−O−H angle (TIP4P-like models). Despite its simplicity, these empirical nonpolarizable rigid models yield very accurate results for a wide variety of properties in the liquid state. The fixed charges produce a permanent molecular dipole which, depending on the model, is around 2.2−2.4 D, clearly larger than the experimental value for the isolated molecule. This is because the many body forces are included in an effective way in the models by modifying the dipole moment μ with respect to that of the gas phase. It is however lower than the "experimental" value.

The dipole moment is, however, only the first term in the multipole expansion.[21] Batista et al. have shown[22] that the electric field obtained from an induction model agrees well with first principles results when the multipole expansion is carried out up to and including the hexadecapole moment and when polarizable dipole and quadrupole moments are included. The SSDQO potential model, which describes a water molecule as a Lennard-Jones sphere with point dipole, quadrupole, and octupole moments, also deserves mention.[23] The quadrupole moment is a tensor, but the off-diagonal components are null in water. Besides, for the usual point-charge water models considered in this work, the diagonal elements may be expressed in terms of a single quantity. Later in this paper, we will discuss this point in more detail, but to simplify the discussion, it is convenient here to refer to this single component as "the quadrupole moment". Despite the intrinsic uncertainty of the results due to the partitioning of the electronic density, ab initio calculations show, in general, that the quadrupole moment is also larger in the liquid[9,10] than that in the gas phase[24,25] (however, in a quantum chemistry study, Tu and Laaksonen[26] found similar results for the quadrupole moment of water in the liquid and gas states). Nevertheless the increase factor of the quadrupole moment in liquid water with respect to that of the water monomer (≈30%) is not as strong as that for the dipole moment (≈60%). Interestingly, a similar enhancement of the quadrupole moment (≈25%) has been reported for ice Ih.[7]

The importance of the quadrupole and higher moments is often neglected. This is probably because the liquid properties (density, internal energy) used to fit the potential models are not sensitive to the relative importance of the dipolar and higher multipolar forces. Thus, the higher multipolar interactions can be effectively accounted for by an increased dipole moment. However, there is clear evidence of the effects of the quadrupolar interactions. In particular, quadrupoles seem to be much more effective than dipoles in orientationally ordering a dense system.[27−29] Besides, it is well-known that the properties of a hard fluid made of point charges differ considerably from those with a point dipole[30−32] due to the effect of higher multipoles in the point-charge system. In the case of water, Carnie and Patey[33] examined a water-like model of hard spheres with embedded dipoles and quadrupoles. This integral equation study showed that the quadrupolar interactions effectively quench the dipolar correlations. As a consequence, the dielectric constant of the liquid decreases considerably as the quadrupole interactions are increased. Similar conclusions have been obtained with more realistic models. In fact, Rick[34] computed the dielectric constant for several water models to conclude that when the dipole moment of the model is enhanced, the dielectric constant increases. However, when the quadrupole moment increases, the dielectric constant drops. Thus, an increase of the dipole moment should be accompanied by a corresponding enhancement of the quadrupole moment of the model (and vice versa) if the dielectric constant is to be accounted for. It also has been reported[35] that the dipolar contributions give sometimes the erroneous sign for the energy differences between ordered and disordered ices (for some configurations in ices Ih/XI and always for ices VII/VIII). When electrostatic terms up to $1/r^6$ are included, the differences have the correct sign. In summary, these examples (and also other reports[36]) give strong indications of the distinctive effect of the dipole and quadrupole in some water properties.

Our analysis of previous studies indicates that (i) the effective value of the dipole moment in ice or liquid water is clearly larger than that for the gas phase, (ii) the effective value of the quadrupole moment in ice and liquid water is probably larger than that for the gas phase, but the enhancement is not as strong as that for the dipole moment, and (iii) the quadrupole interactions effectively quench the dipolar correlations, and thus, a balance between the dipole and quadrupole moments may probably be relevant for certain water properties. Results for polarizable water models and ab initio water simulations are in accordance with the above conclusions. However, the same does not hold for most of the empirical nonpolarizable potentials. We have commented above that the dipole moments of the common empirical water models exhibit an enhancement of the dipole moment; therefore, they are more or less in line with experimental and quantum calculation results. However, the values of the quadrupole moments in these models are systematically lower than the experimental result for the water monomer. This may be because the properties usually investigated seem to be not particularly sensitive to the strength of the quadrupolar interactions since many different orientations are averaged out to contribute to the liquid properties. However, the situation is not necessarily the same for the solid state.

Recently, we have undertaken[37,38] the calculation of the phase diagram involving the different ice polymorphs. One of the conclusions of the study is that the phase diagram is a stringent test for water models. Notice that when considering the performance of a model to describe the phase diagram of water, there are two issues to consider. The first is the prediction of the fluid−solid equilibria: are the melting temperatures of the ices close to the experimental values? The second concerns the relative stability of the different ices, which is related to the solid−solid equilibria: is the general aspect of the phase diagram similar to the experimental one? The first issue involves the stability of the solid with respect to the liquid. The second involves the stability of a certain solid phase with respect to another solid phase. Our studies have shown that TIP4P yields a qualitatively correct phase diagram, while SPC/E and TIP5P (a five center model[39] with a tetrahedral arrangement of charges) do not. For instance, for the latter two models, the thermodynamically stable phase at ambient temperature is not the usual hexagonal ice Ih but ice II. A first analysis of the reasons of the failure of the results for SPC/E indicated that the center of the negative charge should be shifted from the oxygen atom (as in SPC/E) toward the hydrogens (as in TIP4P and derived models). In fact, all of the TIP4P-like models investigated have ice Ih as the stable phase at ambient conditions. The amount of information generated in the last 3 years about the melting point

of different water models and about the aspect of the phase diagram allows one to now analyze, in more detail, the reasons of the success or failure of the different models. Some preliminary results have indicated the existence of a correlation between the melting point of ice Ih and the quadrupole moment.[40] Besides, the results have shown the enormous influence of the ratio of dipolar to quadrupolar forces in the aspect of the phase diagram.[41] However, there are some issues that these preliminary studies do not clarify. First, it is interesting to know whether the melting point of other ices (ice III, V, VI) do also correlate with the quadrupole moment. Second, it is not clear why the aspect of the phase diagram is determined by the ratio of dipolar to quadrupolar forces rather than by the quadrupole moment itself.

In this work, we will attempt to explain the origin of these two findings. The goal of this paper is to achieve a molecular understanding about the phase equilibria (fluid−solid and solid−solid) of water models in relation to the dipolar and quadrupolar forces. It will be shown that for water models with three charges (one negative charge and two positive charges located in the protons), the decision about where to locate the negative charges plays a crucial role. This is so because, as it will be shown, the position of the negative charge determines the relative strength of dipolar and quadrupolar interactions in three-point-charge water models. The conclusions obtained in this work are relevant for all models with three charges, such as SPC, SPC/E, TIP3P, TIP3P-Ew,[42] TIP4P, and the new generation of TIP4P-like models such as TIP4P-Ew,[43] TIP4P/Ice,[44] and TIP4P/2005.[45] The scheme of the paper is as follows. In section II, the equations for the dipole and quadrupole moments of three-point-charge water models are presented. Section III describes the technique used to calculate the phase diagram for a water model from the known phase diagram of a reference model as well as the details of the simulations. In section IV, we examine critically the phase diagram predictions for several popular models and for models with varying dipole and quadrupole moments. Final remarks and the main conclusions (section V) close this paper.

II. Dipole and Quadrupole Moments of Three-Point-Charge Water Models

Despite the great number of proposed models for the water force field,[1] the more popular ones (and, probably, the more successful too) are rigid, nonpolarizable models such as SPC/E, TIP3P, and TIP4P. These empirical potentials were optimized using a small number of properties of liquid water at 298 K as target quantities. The last years have seen the proposal of a number of models (TIP4P-Ew,[43] TIP4P/Ice,[44] and TIP4P/2005[45]), which are reparametrizations of TIP4P based on a wider set of target quantities. These TIP4P-type models have the same functional form as that of TIP4P but with different parameters. As commented in the Introduction, most of these models share a common geometry and functionality, three charged sites and one Lennard-Jones interaction site. Depending on whether the negatively charged center M is coincident with the position of the oxygen atom, the model has three or four interaction sites. However, the expressions for the multipole moments may be written in a general way for these three-point-charge models. In particular, the dipole moment has the form

$$\mu = 2q_H(d_{OH}\cos\theta - d_{OM}) \quad (1)$$

where d_{OM} is the distance between the oxygen and the M site, d_{OH} is the bonding distance, and 2θ is the H−O−H angle.

TABLE 1: Values of the Multipole Moments for Several Rigid Nonpolarizable Models and Their Relation with the Melting Temperature of Ice Ih and with the Relative Stability of Ice II[a]

model	q_H	d_{OM}	μ	Q_T	μ/Q_T	T_m	overstability of ice II
TIP4P/Ice	0.5897	0.1577	2.425	2.434	0.996	272.2	null
TIP4P/2005	0.5564	0.1546	2.305	2.297	1.004	252.1	null
TIP4P-Ew	0.52422	0.125	2.321	2.164	1.073	245.5	medium
TIP4P	0.520	0.150	2.177	2.147	1.014	232.0	null
SPC/E	0.4238	0	2.350	2.035	1.155	215.0	strong
SPC	0.41	0	2.274	1.969	1.155	190.5	strong
TIP3P	0.417	0	2.347	1.721	1.363	146	strong
gas (expt.)	−	−	1.85	2.565	−		−

[a] The charge at the hydrogens is expressed in terms of the proton charge and distance d_{OM} in Å. In TIP4P-like models and TIP3P, the bond length is $d_{OH} = 0.9572$ Å, and the bond angle is $2\theta = 104.52°$, whereas in SPC models, the corresponding values are 1 Å and 109.47°, respectively. Debye units are used for the dipole moment μ, while the quadrupole moment Q_T is given in D·Å. T_m is the melting temperature (in K) of ice Ih for the model, and the last column refers to the degree of overstabilization of ice II in the phase diagram of the corresponding model. Models appear sorted according to their molecular quadrupoles.

Taking the z axis as the bisector of the HOH angle, we may also write it as

$$\mu = 2q_H(z_H - z_M) \quad (2)$$

Table 1 shows the values of dipole moments for popular three-point-charge water models. It is interesting to note the similarity in the dipole moments of the models despite the differences in their hydrogen charges. It seems that the properties used in the fitting of models (particularly, the enthalpy of vaporization and the density of the liquid) almost unequivocally determines the value of the dipole moment whose variations are limited to a quite narrow range. In fact, the difference between the largest and the smallest dipole moments of the potentials models presented in Table 1 is about 10%.

Using a convenient reference system, the quadrupole tensor may be written in a simplified way. A common choice is to make the x axis parallel to the line joining the hydrogens. Thus, y is normal to the molecular plane. In these conditions

$$\mathbf{Q} = \begin{pmatrix} Q_{xx} & 0 & 0 \\ 0 & Q_{yy} & 0 \\ 0 & 0 & Q_{zz} \end{pmatrix} \quad (3)$$

with $Q_{xx} = q_H(2x_H^2 - z_H^2 + z_M^2)$, $Q_{yy} = q_H(-x_H^2 - z_H^2 + z_M^2)$, and $Q_{zz} = q_H(-x_H^2 + 2z_H^2 - 2z_M^2)$. The quadrupole tensor may written in an equivalent way as

$$\mathbf{Q} = \begin{pmatrix} Q_T - \Delta & 0 & 0 \\ 0 & -Q_T - \Delta & 0 \\ 0 & 0 & 2\Delta \end{pmatrix} \quad (4)$$

where $Q_T = (Q_{xx} - Q_{yy})/2$.[33,34,36,46] Q_T has interesting properties in three-point-charge models. First, it is independent of the origin of coordinates

$$Q_T = (3/2)q_H x_H^2 = (3/2)q_H d_{OH}^2 \sin^2\theta \quad (5)$$

It seems then natural to choose an origin for which the quadrupolar tensor may be simply written as

$$\mathbf{Q} = \begin{pmatrix} Q_T & 0 & 0 \\ 0 & -Q_T & 0 \\ 0 & 0 & 0 \end{pmatrix} \quad (6)$$

which is fulfilled with the condition $Q_{zz} = 2\Delta = 0$. Thus

$$(1/2)x'_H{}^2 = z'_H{}^2 - z'_M{}^2 \quad (7)$$

In terms of the bond length and angle, the distance from the oxygen atom to this "natural" origin of coordinates is given by

$$d_{origin} = \frac{d_{OH}\cos\theta + d_{OM}}{2} - \frac{d_{OH}^2 \sin^2\theta}{4(d_{OH}\cos\theta - d_{OM})} \quad (8)$$

It is important to stress that eq 6 is an exact result for this type of model and not an approximation as it is sometimes referred to. This indicates that the quadrupole tensor may expressed in terms of a single component or, in other words, that the strength of the quadrupolar interactions is determined by this quantity, which can be hereafter denoted as "the quadrupole moment". Notice that, as the value of Q_T is independent of the origin of coordinates, it is possible to extract conclusions based on the value of Q_T without being forced to use the coordinates for which eq 6 is fulfilled.

Data in Table 1 show significant differences in the quadrupole moments of three-point-charge water models. The difference between the largest and the smallest quadrupole moments is around 40%, four times larger than that observed for the dipole moments. Besides, a quick look at the table indicates that models with a large departure from the experimental quadrupole (2.565 D·Å) give a poor description of the phase diagram. Later in this paper, we will analyze this question in detail. For the moment, let us conclude this section by pointing out that whereas μ depends on both the hydrogen charge and the position of the negative charge, the quadrupole moment depends only on q_H but not on d_{OM}.

III. The Simulations

In our simulations, the LJ potential is truncated at 8.5 Å, and standard long-range corrections to the LJ energy are added. The Ewald summation technique has been employed for the calculation of the long-range electrostatic forces. For the real-space cutoff, we also employed 8.5 Å. The screening parameter and the number of vectors in the reciprocal space considered was carefully selected for each phase. The sample size for water in the liquid state was 360 water molecules. The number of molecules for the different ice phases was chosen so as to fit at least twice the cutoff distance in each direction. An essential part of the simulations will be devoted to calculate the phase diagram of water models with different dipole and quadrupole moments. In fact, what we calculate are the shifts of the coexistence lines of a reference model due to a change in the potential model. For this, we use the Hamiltonian Gibbs−Duhem integration. The method is a generalization of the integration of the Clapeyron equation sometimes denoted as Gibbs−Duhem integration.[47,48] A description of our implementation can be found in ref 49. For completeness, we sketch here a brief summary of this technique. Let us write a given pair potential in terms of a reference potential as a function of a parameter λ

$$u = (1-\lambda)u_{ref} + \lambda u_{new} \quad (9)$$

When $\lambda = 0$, $u = u_{ref}$, and for $\lambda = 1$, it follows that $u = u_{new}$. We can use λ as a new intensive thermodynamic variable so that a change in the Gibbs free energy per particle is given by

$$dg = -sdT + vdp + x_g d\lambda \quad (10)$$

It can be shown that the conjugate extensive thermodynamic variable x_g is

$$x_g = \frac{1}{N}\left\langle \frac{\partial U(\lambda)}{\partial \lambda} \right\rangle_{N,p,T,\lambda} \quad (11)$$

From this result, following the same steps leading to the classical Clapeyron equation, it is easy to write the generalized relationships

$$\frac{dT}{d\lambda} = \frac{\Delta x_g}{\Delta s} \quad (12)$$

and

$$\frac{dp}{d\lambda} = -\frac{\Delta x_g}{\Delta v} \quad (13)$$

The integration of these equations makes it possible to calculate the shift in the coexistence temperature (or pressure) produced by a change in the interaction potential at constant pressure (or temperature). We have checked that the Hamiltonian Gibbs−Duhem integration results are in very good agreement with the free-energy calculations for the TIP4P and SPC/E models.[49] We have also shown that consistent results for the liquid−ice Ih coexistence temperature of TIP5P are obtained irrespective of the starting potential u_{ref} (TIP4P and SPC/E). Finally, we have also shown that the technique yielded the same results as those of a direct coexistence method[50] for the melting temperatures of ice Ih of SPC/E, TIP4P, TIP4P/Ice, TIP4P/2005, TIP4P-Ew, and TIP5P (and also for a six-site model of water[51]). For the integration of the Hamiltonian Clapeyron equations, a fourth-order Runge−Kutta method algorithm was employed.

IV. Dependence of the Water Phase Diagram on the Dipole and Quadrupole Moments

A. Results for Popular Water Models. *1. General Appearance of the Dense Region of the Phase Diagram.* As commented above, the performance of the rigid nonpolarizable models in the description of the phase diagram involving solid phases is very different. In general, TIP4P-type models yield a qualitatively correct phase diagram (Figure 1a).The exception is TIP4P-Ew (Figure 1b) for which the stability of ice II is overestimated. As a consequence, ice III becomes metastable, and the stability domain of ice V is severely reduced to a small range of temperatures and pressures. Even more serious are the departures from experiment of SPC/E (Figure 1b). There, not only ice III but also ice V are metastable polymorphs. Moreover, for SPC/E, ice Ih is only stable at negative pressures, and therefore, the stable polymorph at ambient conditions is ice II instead.

We may wonder what is the reason of the overstability of ice II in TIP4P-Ew and SPC/E models. A quick analysis[37] pointed unequivocally toward the position of site M, the center of negative charge, as the main responsibility for the failure of the SPC/E phase diagram. We observed that a shift of the M site from its position in TIP4P in the direction of the oxygen atom deteriorated the phase diagram. Given the geometry of the models, such a shift corresponds to an enhancement of the dipole moment. However, the enhancement of the dipole moment cannot be responsible for the deterioration of the phase diagram. Table 1 shows the permanent dipole moment for these models. It is clear that there is no correlation between the overstability of ice II and the strength of the dipolar interactions. In fact, TIP4P (which yields a satisfactory phase diagram) has the smaller dipole moment among all of the models of Table 1.

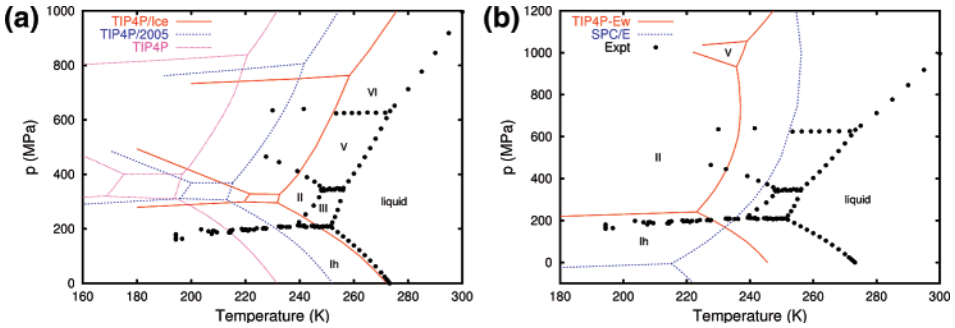

Figure 1. Phase diagram of three-point-charge water models. (a) For models with a μ/Q_T ratio ranging from 0.996 (TIP4P/Ice) to 1.014 Å^{-1} (TIP4P), the labels denote the stable regions of the ice polymorphs in the experimental phase diagram and (by similarity) of the different potential models. Simulation data were taken from refs 37, 44, and 45. (b) For models with $\mu/Q_T = 1.073$ (TIP4P-Ew) and 1.155 Å^{-1} (SPC/E), the labels denote the stable regions of the polymorphs for TIP4P-Ew. The single triple point of the SPC/E diagram is the liquid−Ih−II triple point. Simulation data were taken from refs 37 and 45.

Data in Table 1 show some correlation between Q_T and the relative stability of different ices. It seems that, in general, the anomalously enhanced stability of ice II can be associated with very low values for Q_T. However, the behavior of TIP4P and TIP4P-Ew is somewhat puzzling as Q_T(TIP4P-Ew) > Q_T(TIP4P), while the phase diagram predicted by TIP4P is much closer to experiment than that of TIP4P-Ew. Besides, it is quite surprising that TIP4P, TIP4P/2005, and TIP4P/Ice give a qualitatively similar phase diagram (the main difference between them is a shift toward higher temperatures of the whole diagram) despite the fact that their molecular quadrupoles are sensibly different. If the quadrupolar interactions were invoked to explain the differences in the relative stability of ices, there should be a continuous deterioration along the models shown in Table 1.

The key to solve this puzzle is simple when one remembers that some properties of water (such as the dielectric constant, for instance) result from the compromise between the relative strength of dipole and quadrupole interactions. Up to now, we were not aware of any property that would be distinctly sensitive to the relative strength of dipole and quadrupole interactions; therefore, some models could increment one type of interactions while decreasing the other type. It is clear that the same does not apply to the stability of ices, which seems to be strongly sensitive to the ratio of dipole/quadrupole interactions (see Table 1). In fact, all of the models correctly predicting the relative stability of ices have a μ/Q_T ratio very close to 1.00 (in Å^{-1} units). A small departure from this value (as in TIP4P-Ew) means an overstabilization of ice II, and larger differences lead to unacceptable phase diagrams (as in SPC/E). It is interesting to note that this ratio is similar to that calculated by Batista et al.[7] using an induction model (3.09/3.215 = 0.96 Å^{-1}) and to those obtained in first principle simulations by Delle Site et al.[9] (2.43/2.72 = 0.89 Å^{-1}) and by Silvestrelli et al.[10] (2.95/3.27 = 0.90 Å^{-1}).

It is worth noting that the ratio μ/Q_T depends on d_{OM} (the distance from the M site to the oxygen atom) but not on the molecular charges

$$\frac{\mu}{Q_T} = \frac{4(d_{OH}\cos\theta - d_{OM})}{3(d_{OH}\sin\theta)^2} \tag{14}$$

This ratio can be written in a more compact form in terms of z coordinates in the "natural" origin of coordinates. From eqs 2 and 7, it follows that

$$\frac{\mu}{Q_T} = \frac{2}{3(z'_H + z'_M)} \tag{15}$$

where z'_M is the z coordinate of the M site and z'_H is the z coordinate of the hydrogens' midpoint. The above equation shows that the ratio of the dipole to quadrupole moment in the three-point-charge models is exclusively determined by the position of the negative charge and of the hydrogens' midpoint. As the bond length is very similar in all of the water models, the ratio μ/Q_T is essentially determined by the distance d_{OM}, which differs considerably from model to model.

As a result of our analysis, we may then conjecture that the deterioration of the aspect of the phase diagram may be ascribed to high ratios of dipole/quadrupole moments, which, in turn, are essentially determined by the distance from the oxygen to the negative site. As mentioned in the Introduction, the two issues to consider when investigating the performance of a water model to describe the phase diagram of water are the aspect of the phase diagram (i.e., the relative stability of the different polymorphs) and the liquid−solid envelope (i.e., the prediction of the melting temperatures). Since the first question has been discussed, let us now examine the predictions of the melting temperatures for the different water models to analyze whether they are determined by μ, Q_T, or μ/Q_T.

2. Melting Temperatures of Ices Ih and II. In the previous paragraph, we have shown that the overall appearance of the phase diagram is determined by the relative stability of ice II, which, for some models, takes over other (experimentally) stable polymorphs. Therefore, we have deliberately left aside the question of the liquid−solid envelope. Although the appearance of the phase diagrams of the TIP4P-like models shown in Figure 1a is qualitatively similar to the experimental one, there are some quantitative differences between them. For instance, the results for the melting point of ice Ih of TIP4P, TIP4P/2005 and TIP4P/Ice are 232,[37,38,52,53] 252,[45,50,54] and 272 K,[44,50,54] respectively. It is then interesting to know whether the values of the melting temperatures of three-point-charge models are also dependent on the ratio μ/Q_T. The results for the ice Ih melting temperature at 0.1 MPa (T_m) are shown in Figure 2. In Figure 2a, T_m is displayed as a function of Q_T, and in Figure 2b, it is displayed as a function of μ/Q_T. The correlation observed in Figure 2a is surprisingly good. Unexpectedly, the melting temperature of the models depends almost linearly on Q_T. The melting temperature of hexagonal ice drops for increasing μ/Q_T, but the correlation is far from perfect (Figure 2b). However, the results of Figure 2b clarify the factors affecting the melting point. The results for the models in Figure 2b fall within three families: the TIP4P group with low values of μ/Q_T and high melting points, the SPC family with intermediate values of μ/Q_T and low melting points, and TIP3P with a very large value of μ/Q_T and a very low melting point

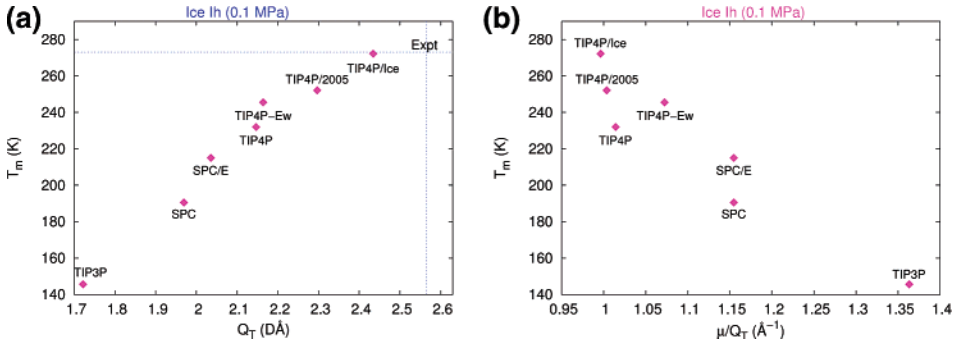

Figure 2. Melting temperature of ice Ih at 0.1 MPa (a) as a function of Q_T and (b) as a function of μ/Q_T.

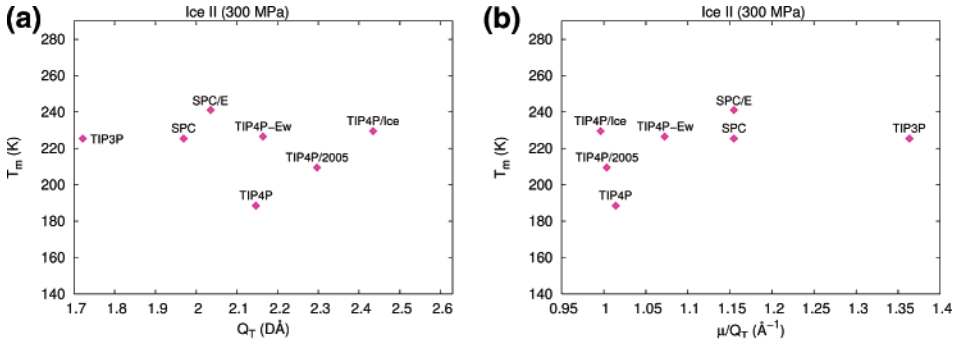

Figure 3. Melting temperature of ice II at 300 MPa for popular three-point-charge water models (a) as a function of Q_T and (b) as a function of μ/Q_T.

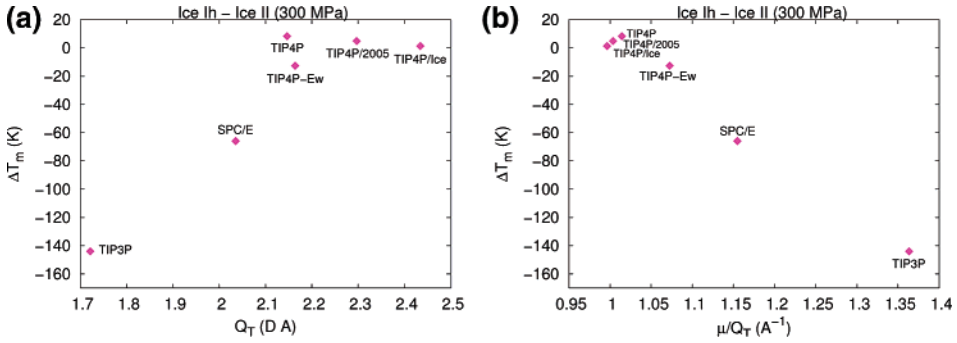

Figure 4. Difference of the melting temperatures of ices Ih and II at 300 MPa (a) as a function of Q_T and (b) as a function of μ/Q_T.

(despite this name, TIP4P-Ew has a μ/Q_T value intermediate between those of the TIP4P and SPC families). Within each family, it is possible to increase the melting temperature by increasing the molecular charges (which increase both the dipole and the quadrupole moments). This explains the higher melting point of TIP4P/Ice with respect to that of TIP4P/2005 and TIP4P. Thus, Figure 2 nicely illustrates the factors affecting the melting point. It is mainly determined by the quadrupolar moment, which, in turn, is dependent (see eq 5) on the magnitude of the molecular charges. Second, it depends on the ratio μ/Q_T, which is related to the way in which the charges are distributed within the model. Figure 2b also indicates that there is no hope in building an SPC-like or TIP3P-like model reproducing the correct melting temperature of ice Ih (i.e., SPC/Ice or TIP3P/Ice models) since, to achieve this goal, a huge charge should be located on the H atoms. For instance, the required hydrogen charge for SPC would produce a dipole moment of about 2.55 D, which seems much too large (the vaporization enthalpy would be around −14.5 kcal/mol to be compared with the experimental value, about −11 kcal/mol). The message from Figure 2b is clear; SPC-like and TIP3P-like models are constrained to have low melting temperatures, and TIP4P/Ice is probably the only choice among the three-point-charge models to reproduce the experimental T_m in a reasonable way.

It is clear from Figure 1a that the melting point of ices III, V, and VI also increase with Q_T similarly to what happens for ice Ih. Thus, it seems that the melting temperatures of the proton-disordered phases Ih, III, V, and VI behave in a quite similar way with respect to changes in the quadrupole moment. An increase in the quadrupole moment provokes an increase in the melting temperature of ices with proton disorder. However, the proton-ordered ice II shows again a peculiar behavior. This different behavior has important consequences. Contrary to what was observed for ice Ih, the melting temperatures of ice II are independent of both Q_T and μ/Q_T (Figure 3). Figure 4 presents the differences of the computed melting temperatures of ices Ih and II at 300 MPa as a function of Q_T (panel a) and μ/Q_T (panel b). Figure 4a shows that, in general, the difference T_m(Ih) − T_m(II) increases with the molecular quadrupole (i.e., its absolute value decreases), but the correlation is far from perfect. On the contrary, the difference decreases almost linearly with the ratio of dipole/quadrupole moment (i.e., its absolute value increases). From eqs 14 and 15, it follows that the relative stability of ices Ih and II depends on the z coordinate of the M

site. Thus, the failure of certain models in accounting for the relative stability of these ice polymorphs is a direct consequence of an inappropriate choice of the position of the negative charge.

In summary, the analysis of the results for the most commonly used water models demonstrate the great sensitivity of the phase diagram to the molecular quadrupole. The correlations found suggest that the melting temperature of ices with proton disorder depends mainly on the magnitude of the quadrupole moment, whereas the relative stability of ice II (where the protons are ordered) with respect to the rest of proton-disordered ices (Ih, III, V, and VI) seems to be correlated with the ratio of dipolar to quadrupolar forces.

B. The Phase Diagram at Constant Geometry and Lennard-Jones Parameters. Throughout this paper, the different performance of the water models to describe the phase diagram of water has been assigned exclusively to the values of the dipole and quadrupole moments. It may be argued that the water models also differ in their LJ and geometrical parameters (bond distances and angles). In order to fully support the conjectures obtained from the discussion presented so far, it would be of interest to analyze models with the same LJ parameters and geometry (i.e., bond distance and angles) and differing exclusively in the values of the dipole or quadrupole moments. The results are presented in this part of the paper. We will perform calculations of the shift (in temperature or pressure) produced by a change in μ, Q_T, or in the ratio μ/Q_T while preserving the rest of the parameters of the model. For this purpose, we shall use the Hamiltonian Gibbs−Duhem integration.[47,55,56] This technique allows examination of the effect in a certain coexistence line produced by a change in the Hamiltonian of the model. As a reference model, we have chosen TIP4P/2005,[45] which has provided excellent results for the whole phase diagram in the high-density region (see Figure 1a). Besides, it describes satisfactorily the temperature of maximum density (278 K),[45] the liquid−vapor equilibria[57] yielding a critical temperature of 640 K (to be compared with the experimental value of 647.1 K), and the surface tension[58] of water. The initial coexistence points for the TIP4P/2005 model are taken from a previous work.[45] Starting at the coexistence point of a given line for TIP4P/2005, we make use of eq 12 or 13 to calculate the coexistence temperature (pressure) for a model with a different pair potential. If the Lennard-Jones parameters (ϵ_{LJ}, σ_{LJ}), and the geometry of the molecule (d_{OH} and θ) are fixed, the quadrupole moment depends exclusively on the hydrogen charge q_H (see eq 5), the ratio of the dipole to quadrupole moment μ/Q_T depends exclusively on the location of the negative charge as given by d_{OM} (eq 14), and the dipole moment depends on both q_H and d_{OM} (eq 1). The following changes are possible (see Table 2): (i) A change in q_H corresponds to a decrease in the quadrupole and dipole moments of the molecule but leaves the ratio μ/Q_T constant. The effect of reducing the charge from $q_H = 0.5564e$ to $q_H = 0.5206e$, leaving the rest of the parameters as those in TIP4P/2005, is shown in Figure 5a. (ii) A change in d_{OM} corresponds to an increase in the dipole moment and in the ratio μ/Q_T but leaves constant the value of the quadrupole moment. The results of the perturbation from $d_{OM} = 0.1546$ to 0.125 are depicted in Figure 5b. (iii) Finally, it is possible to change both q_H and d_{OM} to decrease the value of the quadrupole moment while keeping constant the value of the dipole moment (so that μ/Q_T increases). The effect of a variation from $q_H = 0.5564e$ and $d_{OM} = 0.1546$ to $q_H = 0.5206e$ and $d_{OM} = 0.125$ is shown in Figure 5c.

In Figure 5, the arrows mark the coexistence point of the reference model (TIP4P/2005) and the result for the modified one. As it is shown in Figure 5a, reducing the magnitude of the molecular charges decreases considerably the melting points with respect to the original model but does not modify the aspect of the phase diagram (i.e., it lowers the melting temperatures, but the relative stability of the ices is not effected much). This is in line with the results presented for the popular models of water in the previous section; the melting temperatures are correlated with the quadrupole moment. The fact that the relative stability of ice II with respect to the other ice polymorphs is not changed when the ratio μ/Q_T is kept constant is also in accordance with the conjecture that the ratio of dipolar to quadrupolar forces determines the relative stability of the different ices with respect to ice II. The effect of decreasing d_{OM} at constant q_H (so that Q_T is constant) is shown in panel b. Since the quadrupole moment is constant, the melting points are almost unaffected by the change (notice the small length of the corresponding arrows). However, the coexistence lines where ice II is involved change in a significant way. In particular, the coexistence lines ice II−ice III and ice II−ice V are profoundly effected.

We have shown in Table 1 that common water models have similar dipole moments and differ considerably in their quadrupole moments. Thus, it is interesting to analyze the results of Figure 5c, where the dipole moment is constant and the quadrupole moment is reduced so that the ratio μ/Q_T increases. It can be seen that a variation in the quadrupole moment at constant μ has a great effect in the relative stability of ice II. Notice the large shifts for the ice II−ice III and ice II−ice V coexistence points so that ices III and V become metastable. In fact, the shifts are very similar to those of Figure 5b and much larger than those of Figure 5a. In other words, when the ratio μ/Q_T is increased (by changing μ or Q_T), the range of the stability of ice II increases so that the interval of the stability of ices III, V, and VI is reduced and, eventually, becomes metastable. On the other hand, the melting points of the

TABLE 2: Starting and Final Coexistence Points (Represented by the Arrows in Figure 5) as a Consequence of a Change in the Potential Parameters Modifying the Dipole and/or Quadrupole Moments (LJ Parameters and Bond Length and Angle Are Kept Constant)[a]

	p_i/MPa	T_i/K		T_f/K	
L−Ih	0.1	252.1	200.3	278.9	222.6
L−III	335	214.4	181.8	228.7	193.5
L−V	450	221.9	197.1	228.5	204.1
L−VI	900	248.1	221.9	250.9	228.1
II−III	320	196.5	223.4	330.7	299.4
	T_i/K	p_i/MPa		p_f/MPa	
Ih−II	195	310.0	135.0	271.2	96.7
II−V	199	372.0	235.6	1328	979.8

[a] T_i,T_f (p_i,p_f) indicate the coexistence temperatures (pressures) of the starting and final systems, respectively. The first and second blocks show the coexistence data when the Gibbs−Duhem integration is done at constant pressure and constant temperature, respectively. (For this reason the final pressures or temperatures are not shown.) The starting model is always TIP4P/2005 (μ = 2.305 D, Q_T = 2.297 D·Å, and $\mu/Q_T = 1.004$ Å^{-1}). Column 4 gives the final state for each coexistence point when the molecular charges are reduced to give μ = 2.157 and Q_T = 2.149 (μ/Q_T is the same as that in the starting model) and corresponds to the results shown in Figure 5a. Column 5 gives the final state for each coexistence point when the distance d_{OM} is reduced to give μ = 2.463 and μ/Q_T = 1.072 (Q_T does not change) and corresponds to the results shown in Figure 5b. Column 6 gives the final state for each coexistence point when both the molecular charges and the distance d_{OM} are reduced to give $Q_T = 2.149$ and $\mu/Q_T = 1.072$ (μ is that of the starting model) and corresponds to the results shown in Figure 5c.

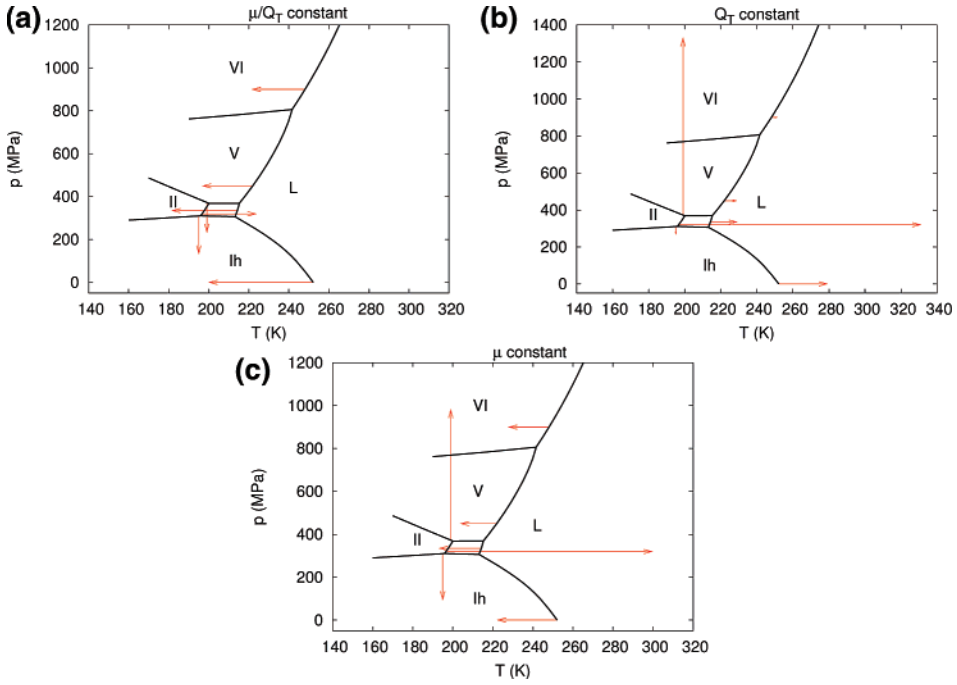

Figure 5. Shifts of some coexistence points as a consequence of a change in the potential parameters modifying the dipole and/or quadrupole moments (bond angle, bond length, and LJ parameters are kept constant). The phase diagram of the starting model (TIP4P/2005) is represented by solid lines. The arrows show the shifts in temperature or pressure of the coexistence points. (a) The hydrogen charge q_H changes from 0.5564 to 0.5206 e (μ and Q_T vary, but μ/Q_T is constant). (b) The distance d_{OM} changes from 0.1546 to 0.125 Å (μ varies at constant Q_T). (c) Both the hydrogen charge q_H and the distance d_{OM} change from 0.5564 to 0.5206 e and from 0.1546 to 0.125 Å, respectively (Q_T varies at constant μ). The numerical values of the starting and final coexistence points as well as the values of μ, Q_T, and μ/Q_T for the starting and final systems of each of the panels are given in Table 2.

disordered polymorphs (Ih, III, V, and VI) move toward lower temperatures by a similar amount. Notice that the shifts in the melting temperatures produced by a change in the quadrupole moment (Figure 5c) are much more important than those produced by a modification of the dipole moment (Figure 5b). In summary, the results of Figure 5 confirm without ambiguity that the quadrupole controls the value of the melting point of proton-disordered ices and that the ratio of dipolar to quadrupolar forces determines the aspect of the phase diagram (i.e., the stability of ice II with respect to the rest of proton-disordered ices).

It is important to note that, since the transformations are not cyclic (the starting potential is the same in the three cases), the variations are not, in principle, additive. However, the results in Figure 5 show that the additivity is almost completely fulfilled, indicating that the shifts depend essentially on the changes in q_H and d_{OM} and are almost independent of the starting potential. Thus, the sum of the changes shown in panels a and b gives essentially the same results as those presented in panel c.

It is interesting to write Q_T as a function of μ

$$Q_T = \frac{3(d_{OH}\sin\theta)^2}{4(d_{OH}\cos\theta - d_{OM})}\mu \qquad (16)$$

This expression is trivially obtained from eq 14. Once the geometry of the water model is imposed (bond length d_{OH} and bond angle 2θ), the quadrupole moment depends exclusively on d_{OM} and μ. If one accepts that a value of the dipole moment around 2.30 D should be used to describe water (as it is in the most popular water models), then d_{OM} plays a key role in determining both Q_T and μ/Q_T. Equation 16 allows discussion of all of the results of this work in a unified form. In fact, we have shown in this paper that, in order to describe correctly the melting point of ice Ih (and that of other proton-disordered ices as III, V, and VI), the value of the quadrupole moment should be close to the experimental gas value. If the dipole moment of the model must be around $\mu = 2.30$ D, then this quadrupole moment can only be achieved with positive values of d_{OM}. In other words, to reproduce the melting point of proton-disordered ices, it is necessary to move the charge from the oxygen toward the hydrogens. We have also shown that, in order to predict successfully the relative stability of ice II, a value of μ/Q_T around 1.0 (or lower) should be used. Within three-charge rigid nonpolarizable models, this is only achieved when the negative charge is located along the H−O−H bisector at a distance of around $d_{OM} = 0.15$ Å. This is the reason why TIP4P-like models provide both a qualitatively correct description of the phase diagram and reasonable melting points, whereas SPC, SPC/E, and TIP3P yield too low melting points and incorrect phase diagram predictions.

Figure 5c showed the shifts of the coexistence points (at constant dipole moment) for a particular change of the distance, namely, $d_{OM} = 0.125$ Å. It seems interesting to calculate the variations of the coexistence properties for a wider range of distances. Figures 6−8 display the evolution of some selected TIP4P/2005 coexistence points when the distance d_{OM} is changed at constant Lennard-Jones and geometric parameters. Since popular water models have similar dipole moments, we focus our attention on the case at constant μ. Thus, associated to the different d_{OM} values, we have also changed the hydrogen charge to keep μ constant (adopting the value of the TIP4P/2005 model). The initial states are the same as the starting points of the arrows in Figure 5. Figure 6 shows how the stability domain of ice III is effected by a change in the ratio of dipole/quadrupole forces. There, we represent the coexistence temperatures of the liquid−ice III, ice II−ice III, and liquid−ice II lines at $p = 300$ MPa for different values of μ/Q_T. The ice II−

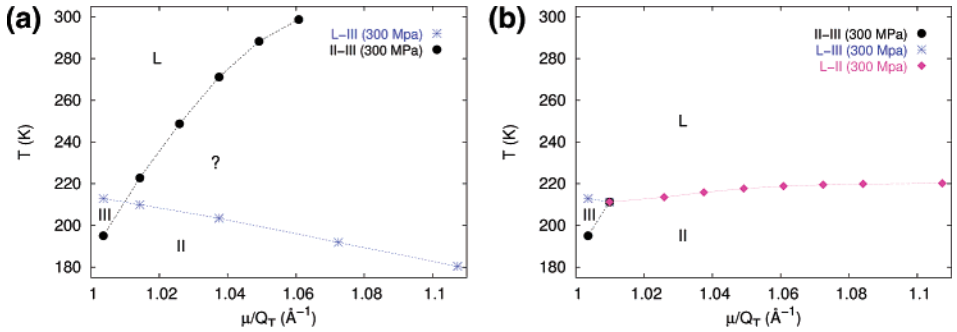

Figure 6. Dependence of the liquid−ice III, ice II−ice III, and liquid−ice II coexistence temperatures at $p = 300$ MPa on the ratio μ/Q_T. The dipole moment μ and Lennard-Jones parameters ϵ_{LJ} and σ_{LJ} are constant and equal to the values for TIP4P/2005. The bond distance angle are those of the TIP4P family. The ratio μ/Q_T is changed by varying d_{OM} and q_H so that the dipole moment remains constant. (a) The melting line of ice II is not taken into account. (b) Stable phases and coexistence temperatures when the ice II melting line is considered.

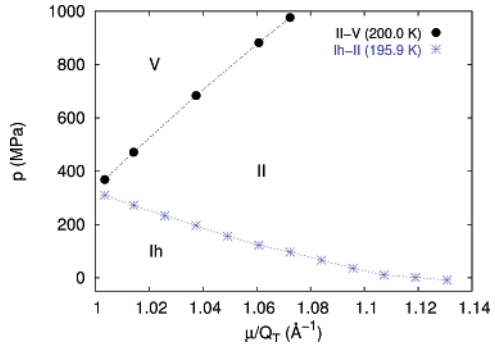

Figure 7. Dependence of the ice II−ice V and ice Ih−ice II coexistence pressures on the ratio μ/Q_T. The dipole moment μ and Lennard-Jones parameters ϵ_{LJ} and σ_{LJ} are constant and equal to the values for TIP4P/2005. The bond distance angle are those of TIP4P-like models.

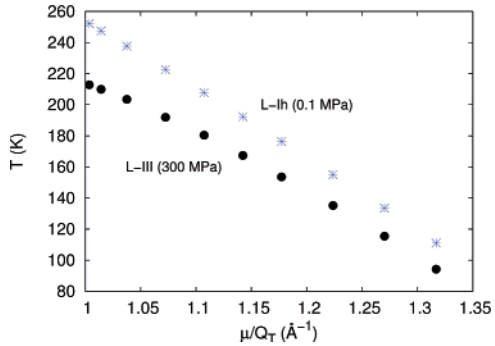

Figure 8. Dependence of the liquid−ice Ih and liquid−ice III coexistence temperatures on the ratio μ/Q_T.

ice III coexistence line (panel a) is strongly sensitive to a small change in the dipole/quadrupole ratio (i.e., the d_{OM} distance) so that the curve has a very large (positive) slope. On the other hand, the ice liquid−ice III coexistence curve has a negative slope; therefore, it crosses the II−ice III coexistence line. Thus, the overall effect of the evolution of the ice II−ice III and liquid−ice III coexistence curves is a strong loss of stability of ice III as the ratio μ/Q_T increases (and, thus, as d_{OM} decreases). The interval of temperatures for which ice III is stable, already very reduced, about 18 degrees, for TIP4P/2005 ($\mu/Q_T = 1.004$ Å^{-1}), vanishes at $\mu/Q_T = 1.010$ Å^{-1}. From that value, the stable polymorph is not ice III but ice II. This explains the absence of ice III in the phase diagrams of TIP4P-Ew ($\mu/Q_T = 1.073$Å^{-1}) and SPC/E ($\mu/Q_T = 1.155$ Å^{-1}). To be complete, Figure 6a would require the inclusion of the liquid−ice II coexistence. We have depicted this panel as is just to realize that the interval of the ratios of dipole/quadrupole yielding acceptable results is quite narrow. Ice III has a reduced stability range (the difference between the liquid−ice III and ice III−ice II coexistence temperatures is always lower than 20°); therefore, its absence in the phase diagram could be forgiven. However, obtaining instead a difference of −70 K (the difference for $d_{OM} = 0.14$ Å which corresponds to $\mu/Q_T = 1.037$ Å^{-1}) is clearly open to objection.

Figure 6b includes the results for the liquid−ice II line. In contrast with the results for the liquid−ice III and ice II−ice III coexistences, the liquid−ice II coexistence temperature is almost independent of μ/Q_T. This is a confirmation of our analysis of the melting temperatures of ice II for popular three-point-charge water models (see Figure 3). Notice finally that the flat aspect of the ice II melting curve should not mask the deterioration of the phase diagram with increasing μ/Q_T, as observed in panel a for the liquid−ice III and ice II−ice III lines.

Figure 7 presents the coexistence pressures for ice Ih−ice II at 195.9 K and ice II−ice V at 200 K as a function of μ/Q_T. The stability domain of ice II strongly grows with μ/Q_T mainly because of the large positive slope of the II−ice V curve. Besides, an increase in μ/Q_T reduces the coexistence pressure of the ice Ih−ice II. This is consistent with the results for TIP4P-Ew for which ice Ih is stable up to about 200 MPa. The curve crosses the zero pressure limit at $\mu/Q_T \approx 1.1$ Å^{-1}. This is in accordance with the fact that, for the SPC/E model, ice Ih is only stable at negative pressures. In summary, as μ/Q_T increases, ice II extends its range of stability at the expense of ice Ih and ice V, especially the latter one. Taking into consideration the shifts of both the ice Ih−ice II and ice II−ice V coexistence pressures, the stability range of ice II increments by about 800 MPa from the initial point up to $\mu/Q_T \approx 1.07$ Å^{-1}. This is again in agreement with the results for TIP4P-Ew. The increase in the coexistence pressure is not enough to make ice V metastable in TIP4P-Ew, though the stability region of ice V is severely reduced in this model. A further increment in the coexistence pressure for larger μ/Q_T explains that ice V becomes metastable in SPC/E.

Finally, Figure 8 show the variation of the liquid−ice Ih coexistence temperature (at 0.1 MPa) compared to that for liquid−ice III. The coexistence curves of both ice polymorphs are almost parallel. This indicates that although the quadrupole moment greatly influences the melting temperatures of ices Ih and III (notice the negative slope of the curves), it does not affect the relative stability of these ices. Similar shifts have been obtained (results not shown) for the liquid−ice V and liquid−ice VI coexistence curves. The conclusion is that an increase

in μ/Q_T extends the stability of the liquid phase and reduces that of the disordered ices, but the relative stability of the ices with proton disorder (Ih, III, V, and VI) is not modified significantly. In other words, when the quadrupole moment is reduced, the overall liquid−solid envelope is simply shifted toward lower temperatures. Thus, the correlation observed in Figure 2 between the melting temperature and the quadrupole moment does not only apply to ice Ih but also to the rest of the ices with proton disorder (III, V, and VI).

It is worth finishing the results section with a comment about the energy differences responsible for the spectacular deviations reported for the phase diagram. In 1987, Handa, Klug, and Whalley[59] determined the relative energies of the ices at zero pressure for a temperature close to 150 K from calorimetric measurements. Taking ice II as a reference, the relative energies of ices Ih, III, V, and VI are (in kcal/mol) 0.004, 0.230, 0.235, and 0.352, respectively.[59,60] Notice that, at these conditions, ice II is marginally more stable than ice Ih and that the energy differences are quite small. Recently, we have carried out a similar study for the energy differences of popular water models.[60] In particular, TIP4P/2005 yields results close to the experiment for all of the disordered ices, although ice Ih is predicted to be more stable than ice II (−0.209, 0.112, 0.218, and 0.338 kcal/mol, respectively). In accordance with the results of this paper, SPC/E predicts a strong overstabilization of ice II since all of the relative energies are positive and considerably higher than the experimental data: 0.164, 0.511, 0.704, and 0.918 kcal/mol, respectively.

V. Discussion and Conclusions

Simple empirical three-point-charge water models such as TIP3P, SPC/E, and TIP4P are quite successful in describing the properties of water. It is only in the solid phase where we find that the performance of these models is different in a significant way. In this work, we have attempted to relate their different ability to describe the phase diagram of water (fluid−solid and solid−solid) equilibria to the dipole and quadrupole moments of the water models. The analysis of the effect of the quadrupole can be greatly simplified by an adequate choice of the reference system. We have shown that it is possible to define a single scalar quantity Q_T as a representative measure of the strength of the quadrupolar forces much in the same way as the modulus of the dipole moment is used to give an idea of the strength of the dipolar forces. In this way, we have been able to describe the dependence of the first multipole moments on the potential parameters. For a given molecular geometry (bond length and angle), the dipole moment is a function of both the magnitude of the hydrogen charge and the position of the negative charge, but the quadrupole moment depends only on the magnitude of the charges and the ratio of dipole/quadrupole on the position of the negative charge.

Our initial analysis clearly pointed to the important role played by the quadrupolar forces. However, the way in which the quadrupole affects the phase diagram seems to be double. On the one hand, the melting temperatures of proton-disordered ices such as Ih, III, V, and VI show a strong correlation with the molecular quadrupole. On the other hand, the general aspect of the phase diagram rather depends on the ratio of dipolar/quadrupolar forces. In fact, the deterioration of the phase diagram for some water models could be ascribed to the increase of the ratio of dipolar/quadrupolar forces. These conclusions were obtained by examining the results for several popular models of water. However, since these models differ also in the LJ parameters or even in geometrical parameters such as the O−H bond length, it was of interest to provide clear evidence of this suggestion. For this reason, in this work, we have carried out some calculations for systems at constant geometry and Lennard-Jones parameters and varying q_H and/or d_{OM}. In this way, we have confirmed unambiguously that a decrease of the distance d_{OM} (which modifies the dipole/quadrupole ratio) strongly enhances the stability of ice II with respect to ices Ih, III, and V. Good phase diagram predictions are obtained only when the ratio μ/Q_T is relatively close to 1.0 $Å^{-1}$. We have also shown that to obtain models with a melting temperature relatively close to the experimental value, the quadrupole moment of the water model should be close to the experimental one. For three-point-charge models, this can only be achieved when the negative charge is shifted from the oxygen along the H−O−H bisector.

Throughout this work, we have put the emphasis on a basic physicochemical question, namely, the effect of dipolar and quadrupolar interactions on the phase diagram. It is evident that our analysis also involves more practical issues. Regarding the effective dipole moment, there is considerable agreement on values around 2.30−2.35 D. This work provides a minor hint to this question; our results give a new argument supporting the inclusion of the self-polarization energy in the calculation of the enthalpy of vaporization pioneered by the authors of SPC/E. The improvement of the SPC/E predictions with respect to those for SPC involves a great number of water properties. In this work, we add a new property to the list. We show that the melting temperatures are significantly closer to experiment when the dipole moment of the model is increased to take into account the self-polarization term (for instance, SPC vs SPC/E and TIP4P(original) vs new generation TIP4P-like models). However, the more important results of this work concern the effective quadrupole moment. In particular, the mapping of the ratio μ/Q_T onto the d_{OM} distance and the sensitivity of the aspect of the phase diagram to these quantities implies some constraint on the position of the negative charge. According to our results for three-point-charge models, the distance from the negative charge to the oxygen atom should be larger than about 0.14 Å if a qualitative agreement with the experimental phase diagram is desired. Taking into consideration the constancy in the dipole moments of popular water models, this leads to an effective quadrupole moment of around 2.3 D·Å. It is clear that our conclusion concerns only the effective dipole and quadrupole moments of rigid nonpolarizable models. However, as shown above, the "experimental" ratio μ/Q_T obtained by Batista et al. is 0.96 $Å^{-1}$, quite close to the value (around 1.0 $Å^{-1}$) required for three-point-charge models to yield a satisfactory phase diagram. Finally, let us note that although the conclusions of this study cannot be strictly applied to other molecular geometries, there are some indications of a more general validity. For example, the failure of the predictions yielded by TIP5P[49] are consistent with a similar scenario. It has a dipole moment in line with those of three-point-charge models (2.29 D) and a smaller Q_T (1.56 D·Å), and thus, the high value of the ratio μ/Q_T (1.46 $Å^{-1}$) would be at the origin of the bad results for the phase diagram of TIP5P. In other words, it seems that the phase diagram does not support the placement of the negative charges beyond the oxygen atom even if they are split into two separated charges at the presumed positions of the "lone pair" electrons as in TIP5P.

All of the evidence of this work shows that the quadrupole moment of water and the ratio μ/Q_T should be restricted to a narrow range in order to yield satisfactory phase diagrams. What remains to be explained is why the phase diagram is so sensitive

to the quadrupole moment while many other properties are not. It is in accordance with what we learned in secondary school that the melting temperatures of ices Ih and III decrease when the intermolecular interactions are weakened; if the dipole or quadrupole moments are lowered, the result is a decrease of the melting point. It seems more difficult to explain the dependence of the aspect of the phase diagram on the ratio of dipolar/quadrupolar forces. It is well-known that the polar interactions give rise to preferred orientations between the molecules. However, the preferred orientations are not the same for the different terms of the multipole expansion. It has been reported that, as cooperative effects are allowed to be expressed, the relative energy contributions from the dipole and the quadrupole change, with possibly significant consequences for the orientational structure.[27,28,33] Thus, the final preferred orientations result from the balance between the more important terms of the multipole expansion and the thermal motion. In the liquid, thermal motion favors many different relative orientations of the water molecules. The averaging of these orientations explains that the thermodynamic properties of the liquids can be sensitive to the total electrostatic contribution but not to the relative strength of the successive multipole terms. The results for some properties, such as the dielectric constant, that depend on the molecular orientations are illustrative. As shown by Rick,[34] it is possible to balance (within some reasonable limits) the contributions of the dipolar and quadrupolar forces in liquid water in order to yield, more or less, satisfactory dielectric constants. In summary, potential models with a different balance of dipolar and quadrupolar forces may behave similarly in the description of the liquid state, provided that the total electrostatic contribution is adequately accounted for. However, the situation is different for the solid phases[61] because the molecules have fixed lattice positions.

In this work, we have shown that for ices with proton disorder (in which the relative orientations are not fixed), the reduction of the quadrupole provokes a decrease in the melting point. This is the case of ices Ih, III, V, and VI. Probably, the quadrupolar interactions are more favorable in these ices than those in water so that the reduction of the quadrupole moment affects the ices to a greater extent and provokes the "loss of territory" with respect to the liquid in the phase diagram (the east front). However, bad news never come alone. In ice II, the protons are ordered, and the reduction of the quadrupole moment provokes a different response. In fact, the stability of ice II with respect to the rest of the ices is strengthened when one reduces the magnitude of the quadrupole moment. It is likely that the quadrupolar energy is less favorable in ice II (where the orientations are fixed) so that the reduction of the quadrupole enhances the stability of ice II with respect to the disordered ices. Thus, when the magnitude of the quadrupole moment of water is reduced, the region in the phase diagram occupied by ice Ih is reduced by both the liquid (east front) and by ice II (north front) eventually disappearing from the phase diagram as a stable phase. The fact that the stability of a proton-ordered phase such as ice II changes in a different way to those with proton disorder is probably not unique to ice II, but it is likely that it also occurs for other phases where the protons are ordered[61,62] (i.e., ice VIII, IX, ...). Also, the investigation of the stability of ice I ordered phases (ferroelectric and antiferroelectric) could also be of great interest. However, it is also possible that ice II has special features (not necessarily related to its proton-ordered structure) that make its stability different from that of the other polymorphs. More studies would be required to assess this issue.

We would like to point out finally that the atom−atom distribution functions of the ordered ices seem also particularly sensitive to the details of the models.[63,64] Unfortunately, no experimental data are available to check whether the structural information is in line with the conclusions of this work. It has been suggested since some time ago that solid phases could be used to improve our current models of water.[27,65,66] It has also been pointed out that the quadrupole plays an important role in determining water properties.[27,28,33,34,67] In this work, these ideas are put in action, and it is shown how the quadrupolar forces indeed play an important role in understanding water and how they are crucial in understanding the phase diagram of water.

Acknowledgment. This work has been supported by Grants FIS2004-02954-C03-02 and FIS2007-66079-C02-01 of D.G.I. (Spain) and S-0505/ESP/0299 of the Comunidad de Madrid.

References and Notes

(1) Guillot, B. *J. Mol. Liq.* **2002**, *101*, 219.
(2) Matsuoka, O.; Clementi, E.; Yoshimine, M. *J. Chem. Phys.* **1976**, *64*, 1351.
(3) Saint-Martin, H.; Hess, B.; Berendsen, H. J. C. *J. Chem. Phys.* **2004**, *120*, 11133.
(4) Saint-Martin, H.; Hernandez-Cobos, J.; Bernal-Uruchurtu, M. I.; Ortega-Blake, I.; Berendsen, H. J. C. *J. Chem. Phys.* **2000**, *113*, 10899.
(5) Svishchev, I. M.; Kusalik, P. G.; Wang, J.; Boyd, R. J. *J. Chem. Phys.* **1996**, *105*, 4742.
(6) Coulson, C. A.; Eisenberg, D. *Proc. R. Soc. London, Ser. A* **1966**, *291*, 445.
(7) Batista, E. R.; Xantheas, S. S.; Jönsson, H. *J. Chem. Phys.* **1998**, *109*, 4546.
(8) Gubskaya, A. V.; Kusalik, P. G. *J. Chem. Phys.* **2002**, *117*, 5290.
(9) Delle Site, L.; Alavi, A.; Lynden-Bell, R. M. *Mol. Phys.* **1999**, *96*, 1683.
(10) Silvestrelli, P. L.; Parrinello, M. *J. Chem. Phys.* **1999**, *111*, 3572.
(11) Rick, S. W.; Stuart, S. J.; Berne, B. J. *J. Chem. Phys.* **1994**, *101*, 6141.
(12) Yu, H.; Hansson, T.; van Gunsteren, W. F. *J. Chem. Phys.* **2003**, *118*, 221.
(13) Paricaud, P.; Předota, M.; Chialvo, A. A.; Cummings, P. T. *J. Chem. Phys.* **2005**, *122*, 244511.
(14) Petrenko, V. F.; Whitworth, R. W. *Physics of Ice*; Oxford University Press: Oxford, U.K., 1999.
(15) Finney, J. L. *Philos. Trans. R. Soc. London, Ser. B* **2004**, *359*, 1145.
(16) Berendsen, H. J. C.; Postma, J. P. M.; van Gunsteren, W. F.; Hermans, J. In *Intermolecular Forces*; Pullmann, B., Ed.; Reidel: Dordrecht, The Netherlands, 1981; pp 331−342.
(17) Berendsen, H. J. C.; Grigera, J. R.; Straatsma, T. P. *J. Phys. Chem.* **1987**, *91*, 6269.
(18) Jorgensen, W. L. *J. Am. Chem. Soc.* **1981**, *103*, 335.
(19) Jorgensen, W. L.; Chandrasekhar, J.; Madura, J. D.; Impey, R. W.; Klein, M. L. *J. Chem. Phys.* **1983**, *79*, 926.
(20) Bernal, J. D.; Fowler, R. H. *J. Chem. Phys.* **1933**, *1*, 515.
(21) Carlevaro, C. M.; Blum, L.; Vericat, F. *J. Chem. Phys.* **2003**, *119*, 5198.
(22) Batista, E. R.; Xantheas, S. S.; Jonsson, H. *J. Chem. Phys.* **2000**, *112*, 3285.
(23) Ichiye, T.; Tan, M. L. *J. Chem. Phys.* **2006**, *124*, 134504.
(24) Verhoeven, J.; Dymanus, A. *J. Chem. Phys.* **1970**, *52*, 3222.
(25) Gray, C. G.; Gubbins, K. E. *Theory of Molecular Fluids*; Clarendon Press: Oxford, U.K., 1984.
(26) Tu, Y.; Laaksonen, A. *Int. J. Quantum Chem.* **2005**, *102*, 888.
(27) Finney, J. L.; Quinn, J. E.; Baum, J. O. In *Water Science Reviews 1*; Franks, F., Ed.; Cambridge University Press: Cambridge, U.K., 1985.
(28) Patey, G. N.; Valleau, J. P. *J. Chem. Phys.* **1976**, *64*, 170.
(29) Vega, C.; Monson, P. A. *J. Chem. Phys.* **1995**, *102*, 1361.
(30) Lomba, E.; Lombardero, M.; Abascal, J. L. F. *J. Chem. Phys.* **1989**, *91*, 2581.
(31) Lomba, E.; Lombardero, M.; Abascal, J. L. F. *Mol. Phys.* **1989**, *68*, 1067.
(32) Morriss, G. P.; Cummings, P. T. *Mol. Phys.* **1982**, *45*, 1099.
(33) Carnie, S. L.; Patey, G. N. *Mol. Phys.* **1982**, *47*, 1129.
(34) Rick, S. W. *J. Chem. Phys.* **2004**, *120*, 6085.
(35) Tribello, G. A.; Slater, B. *Chem. Phys. Lett.* **2006**, *425*, 246.
(36) Tan, M. L.; Lucan, L.; Ichiye, T. *J. Chem. Phys.* **2006**, *124*, 174505.
(37) Sanz, E.; Vega, C.; Abascal, J. L. F.; MacDowell, L. G. *Phys. Rev. Lett.* **2004**, *92*, 255701.

(38) Sanz, E.; Vega, C.; Abascal, J. L. F.; MacDowell, L. G. *J. Chem. Phys.* **2004**, *121*, 1165.
(39) Mahoney, M. W.; Jorgensen, W. L. *J. Chem. Phys.* **2000**, *112*, 8910.
(40) Abascal, J. L. F.; Vega, C. *Phys. Chem. Chem. Phys.* **2007**, *9*, 2775.
(41) Abascal, J. L. F.; Vega, C. *Phys. Rev. Lett.* **2007**, *98*, 237801.
(42) Price, D. J.; Brooks, C. L. *J. Chem. Phys.* **2004**, *121*, 10096.
(43) Horn, H. W.; Swope, W. C.; Pitera, J. W.; Madura, J. D.; Dick, T. J.; Hura, G. L.; Head-Gordon, T. *J. Chem. Phys.* **2004**, *120*, 9665.
(44) Abascal, J. L. F.; Sanz, E.; García Fernández, R.; Vega, C. *J. Chem. Phys.* **2005**, *122*, 234511.
(45) Abascal, J. L. F.; Vega, C. *J. Chem. Phys.* **2005**, *123*, 234505.
(46) Carnie, S. L.; Chan, D. Y. C.; Walker, G. R. *Mol. Phys.* **1981**, *43*, 1115.
(47) Kofke, D. A. *J. Chem. Phys.* **1993**, *98*, 4149.
(48) Kofke, D. A. *Mol. Phys.* **1993**, *78*, 1331.
(49) Vega, C.; Sanz, E.; Abascal, J. L. F. *J. Chem. Phys.* **2005**, *122*, 114507.
(50) García Fernández, R.; Abascal, J. L. F.; Vega, C. *J. Chem. Phys.* **2006**, *124*, 144506.
(51) Abascal, J. L. F.; García Fernández, R.; Vega, C.; Carignano, M. A. *J. Chem. Phys.* **2006**, *125*, 166101.
(52) Gao, G. T.; Zeng, X. C.; Tanaka, H. *J. Chem. Phys.* **2000**, *112*, 8534.
(53) Koyama, Y.; Tanaka, H.; Gao, G.; Zeng, X. C. *J. Chem. Phys.* **2004**, *121*, 7926.
(54) Vega, C.; Martin-Conde, M.; Patrykiejew, A. *Mol. Phys.* **2006**, *104*, 3583.
(55) Agrawal, R.; Kofke, D. A. *Mol. Phys.* **1995**, *85*, 23.
(56) Camp, P. J.; Mason, C. P.; Allen, M. P.; Khare, A. A.; Kofke, D. A. *J. Chem. Phys.* **1996**, *105*, 2837.
(57) Vega, C.; Abascal, J. L. F.; Nezbeda, I. *J. Chem. Phys.* **2006**, *125*, 034503.
(58) Vega, C.; de Miguel, E. *J. Chem. Phys.* **2007**, *126*, 154707.
(59) Handa, Y. P.; Klug, D. D.; Whalley, E. *Can. J. Chem.* **1988**, *66*, 919.
(60) Aragonés, J. L.; Noya, E. G.; Abascal, J. L. F.; Vega, C. *J. Chem. Phys.* **2007**, accepted.
(61) Rick, S. W. *J. Chem. Phys.* **2005**, *122*, 94504.
(62) Vega, C.; Abascal, J. L. F.; Sanz, E.; MacDowell, L. G.; McBride, C. *J. Phys.: Condens. Matter* **2005**, *17*, S3283.
(63) Vega, C.; McBride, C.; Sanz, E.; Abascal, J. L. F. *Phys. Chem. Chem. Phys.* **2005**, *7*, 1450.
(64) Martin-Conde, M.; MacDowell, L. G.; Vega, C. *J. Chem. Phys.* **2006**, *125*, 116101.
(65) Morse, M. D.; Rice, S. A. *J. Chem. Phys.* **1982**, *76*, 650.
(66) Whalley, E. *J. Chem. Phys.* **1984**, *81*, 4087.
(67) Watanabe, K.; Klein, M. L. *Chem. Phys.* **1989**, *131*, 157.